Valence-band structure of highly efficient *p*-type thermoelectric PbTe-PbS alloys

Christopher M. Jaworski,[1] Michele D. Nielsen,[1] Hsin Wang,[2] Steven N. Girard,[3] Wei Cai,[2] Wally D. Porter,[2] Mercouri G. Kanatzidis,[3] and Joseph P. Heremans[1,4]

[1]*Department of Mechanical and Aerospace Engineering, The Ohio State University, Columbus, Ohio 43210, USA*
[2]*High Temperature Materials Laboratory, Oak Ridge National Laboratory, Oak Ridge, Tennessee 37831, USA*
[3]*Department of Chemistry, Northwestern University, Evanston, Illinois 60208, USA*
[4]*Department of Physics, The Ohio State University, Columbus, Ohio 43210, USA*

(Received 17 August 2012; revised manuscript received 26 October 2012; published 4 January 2013)

Experimental evidence is given relevant to the temperature dependence of the valence band structure of PbTe and $PbTe_{1-x}S_x$ alloys ($0.04 \leqslant x \leqslant 0.12$), and its effect on the thermoelectric figure of merit ZT. The $x = 0.08$ sample has $ZT \sim 1.55$ at 773 K. The magnetic field dependence of the high-temperature Hall resistivity of heavily p-type ($>10^{19}$ cm^{-3}) Na-doped $PbTe_{1-x}S_x$ reveals the presence of high-mobility electrons. This casts doubts on prior analyses of the Hall coefficient suggesting that temperature induces a rapid rise in energy of the "heavy" hole relative to the "light" hole bands. The electron-like behavior is likely induced by the topology of the Fermi surface when the L- and Σ-bands merge. Negative values for the low-temperature thermopower are also observed. The data show that PbTe continues to be a direct-gap semiconductor at temperatures where the ZT and $S^2\sigma$ of p-type PbTe are optimal, e.g., 700–800 K.

DOI: 10.1103/PhysRevB.87.045203 PACS number(s): 71.20.Nr, 72.20.My, 72.20.Pa

I. INTRODUCTION

PbTe[1,2] and its alloys with PbS[3,4] are the materials with some of the highest thermoelectric figures of merit in the temperature range of 550–750 K suitable for waste heat recovery applications.[5] The figure of merit of a material is $ZT = TS^2\sigma/\kappa$, where S is the material's thermopower or Seebeck coefficient, κ is its thermal conductivity, $\sigma = 1/\rho$ is its electrical conductivity (ρ = resistivity), and T is the absolute temperature. Binary PbTe, both p-type[6] and n-type,[7] can be doped to yield thermoelectric figures of merit ZT at 750 K exceeding $ZT \sim 1.4$. The main reasons for this are the favorable power factor $S^2\sigma$ and low lattice thermal conductivity. In n-type material, the power factor benefits from the good mobility that results from the high dielectric constant that screens much of the impurity scattering. The power factor can be high in heavily doped ($\gtrsim \sim 4 \times 10^{19}$ cm^{-3}) p-type material because of the complex valence band structure: The Fermi surface of heavily doped p-type material can include numerous pockets. Screening of impurity scattering also is effective here. The low lattice thermal conductivity of even binary PbTe is due to the high anharmonicity of the bonds, which results in intense phonon-phonon scattering at high temperature. The recently identified[8,9] soft behavior of the PbTe the lattice is related to this anharmonicity, which in turn can be ascribed to the lone-pair s-electrons of divalent Pb.[10] This behavior was also identified in PbSe and PbS.[8] An incipient phase transition of possibly a similar nature is also present[11] in the $PbTe_{1-x}S_x$ alloys studied here, and bodes well for their thermoelectric performance.

Some of the established literature reports a crossing of the light and heavy hole bands of PbTe below the operating temperature range of thermoelectric devices. It has thus been stated,[1] including by authors of the present article,[3] that PbTe is an indirect-gap semiconductor at temperatures where the ZT and $S^2\sigma$ of p-type PbTe are optimal by virtue of the rapid rise in energy of the so-called "heavy" lower valence band (LVB) relative to the "light" upper valence band (UVB). In this paper, we present experimental evidence to the contrary. We start with a review of the literature that highlights weaknesses in the historical evidence that PbTe, a direct-gap semiconductor at low T, becomes an indirect-gap one with two sections of the valence band crossing at $T_0 \sim 415$ K. We then report transport data that shed light on the T-dependent Hall coefficient ($R_H[T]$) measurements. The results are obtained on heavily doped p-type state-of-the-art samples that exhibit $ZT \sim 1.55$ at $670\,\text{K} < T < 750\,\text{K}$, and show that at 600 K, $R_H(T)$ is not a good measurement of the hole concentration because it contains a substantial contribution from high-mobility minority electrons. A possible origin is suggested for this electron-like behavior: It is likely a topological feature of the Fermi surface at hole concentrations where the carriers at the L-point and those around the Σ-points merge.[12] This is a feature similar to that in the Fermi surface of copper, which is responsible for the positive polarity of its thermopower. It is also possible that an impurity band forms due to the high Na concentrations. Revisiting the analysis of the Hall data in the light of these features suggests that high ZT values are obtained in PbTe at temperatures where it continues to be a direct-gap semiconductor. This conclusion does not distract from the fact that the holes in the heavy LVB pockets play an important role in the final ZT, whether they result from a very high chemical doping level, or are thermally induced in less-doped samples.

II. LITERATURE

A review of the experimental evidence for the crossing of two parts of the valence band of PbTe with increasing temperature is necessary to put the present work in context. The band structure of PbTe has been long established experimentally at cryogenic temperatures with Fermi surface mapping techniques such as de Haas van Alphen, Shubnikov–de Haas, and magneto-optics, and calculations[12] are consistent with the experiments. The valence band of PbTe consists[12] of a "light" UVB at the four L-points of the Brillouin zone,

and a "heavy" LVB broadly distributed over the zone near the Σ-points and between the L- and Σ-points; at a p-type doping level in the mid-10^{19} cm^{-3} range, the Fermi surfaces of these two bands merge together. At low temperature, PbTe is unambiguously a direct-gap semiconductor, with a gap located at the L-point of the Brillouin zone. As long as the Fermi level (ε_F) does not reach the LVB, the conduction (CB) and valence (the UVB) bands are nearly symmetrical and have a small effective mass (at 4 K $m^*_{\|[111]} \sim 0.24 \pm 0.05\, m_e$; $m^*_{\perp[111]} \sim 0.023 \pm 0.001\, m_e$; $m^*_{\rm DOS} \sim 0.13\, m_e$ at the band edge)[12] and high mobility. The absolute values of the thermopower of n-type[14,15] and UVB-dominated p-type[16] materials, when plotted versus carrier concentration at 300 K, are almost identical. The mobility of UVB holes is less than that of electrons. The direct energy gap is given by:[17]

$$\varepsilon_g(T) = 171 + \sqrt{164 + 0.19(T + 20)^2}\ \text{meV}, \qquad (1)$$

and, at $T > 100$ K, it increases nearly linearly with T with $d\varepsilon_g/dT \sim 0.41$ to 0.45 meV K^{-1}.[13] Bands move little with T for $T < 80$ K because the main origin of the temperature dependence of the band structure is the lattice expansion, and thermal expansion decreases rapidly below the Debye temperature. Because this small energy gap is determined by spin-orbit interactions, the UVB and CB are strongly nonparabolic and follow a Dirac-like dispersion, with effective masses that increase as a function of energy ε into the bands following approximately:[18]

$$m^*(\varepsilon) = m^*(\varepsilon = 0)(1 + 2\varepsilon/\varepsilon_g). \qquad (2)$$

At low temperature ($T < 80$ K), the energy separation between the maxima of the UVB and the LVB is $\Delta\varepsilon_v(0\,\text{K}) = 160{-}170$ meV.[19,20] The Fermi surfaces of degenerately doped samples with enough carriers to reach the LVB look like a series of tubes arranged along the edges of a cube inscribed inside the Brillouin zone.[12] The density of states in the LVB is much higher than in the UVB, with a DOS mass of the order of $m^*_{\rm DOS-LVB} \sim 0.6$ to $2.5\, m_e$.[13] This gives the LVB holes a higher thermopower than the UVB holes, and thus it is favorable to ZT to have ε_F in the LVB. At operating temperatures of thermoelectric devices near 600 K, the LVB of heavily doped ($p > 5 \times 10^{19}$ cm^{-3}) PbTe is populated and contributes to the high ZT of the material at these temperatures, as has been described previously.[1,3,12]

PbS has a band structure almost identical to PbTe, with a slightly larger direct L-point energy gap, but a very similar temperature dependence (as does PbSe):[17]

$$\varepsilon_g = 263 + [400 + 0.265\, T^2]^{1/2}\ \text{meV}. \qquad (3)$$

The position of the LVB, and its temperature dependence, is less well established than for PbTe, and it is estimated at $\Delta\varepsilon_v > 300$ meV at 0 K.[20]

The transport properties of the valence band of heavily p-type doped $Pb_{1-y}Na_yTe$ have been extensively investigated[16,21–24] and are summarized by Ravich *et al.*[18] The temperature dependence of $\Delta\varepsilon_v(T)$ is such that at T above some temperature T_0, defined by $\Delta\varepsilon_v(T_0) = 0$, PbTe turns into an indirect-gap semiconductor with the CB minimum at the L-point, and the maximum of the valence band is the LVB. Two

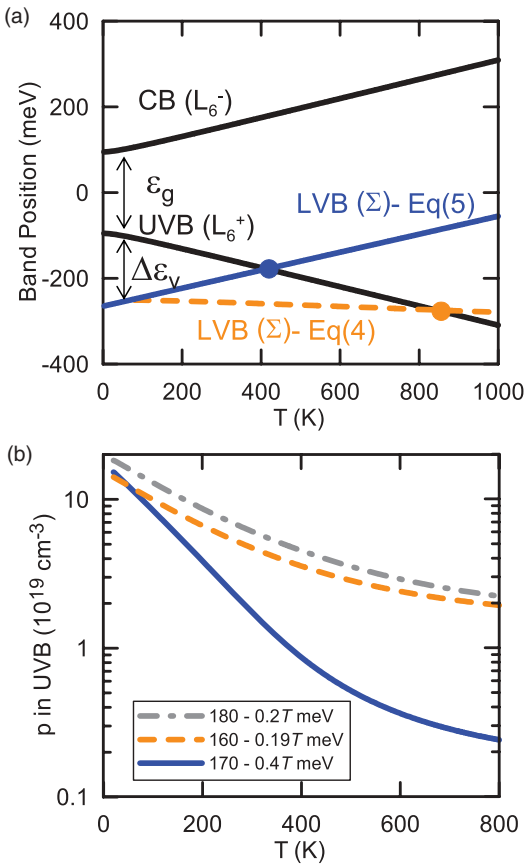

FIG. 1. (Color online) (a) Schematic temperature dependencies of the relative positions of the different bands of PbTe. The bands are the CBs and UVBs at the L-point, and a LVB in a pocket near the Σ-points. Two temperature dependencies are proposed in the literature for the relative positions of the UVB and LVB, which are separated by $\Delta\varepsilon_v$. The latter is given by either Eq. (4) or Eq. (5); see text. (b) Calculated density of holes in the UVB for the proposed temperature dependencies of $\Delta\varepsilon_v(T)$.

very different temperature dependencies for $\Delta\varepsilon_v(T)$ above about 80 K are reported in the literature [Fig. 1(a)].

1. Allgaier and Houston[25] suggest and Rogers[19] reformulates ($T > 80$ K):

$$\Delta\varepsilon_v(T) \sim 160\,\text{meV} - 2.2k_BT = 160 - 0.19T\ \text{meV}, \qquad (4)$$

which is shown as the orange line in Fig. 1(a). Independent of this work, Airapetyants[16] proposes a similar formula:

$$\Delta\varepsilon_v(T) \sim 180 - 0.2T\ \text{meV}. \qquad (4a)$$

This is not shown in Fig. 1(a) for clarity due to its similarity with Eq. (4). If Eq. (4) holds, $T_0 \sim 800$ K, and the band crossing does not play a role in the ZT of p-type PbTe at operating temperatures, although the concentration of thermally induced or chemically placed holes in the LVB is still important at $T > 600$ K.

2. In contrast, Refs. 1, 18, 21, and 26–28 report, for $T > 80$ K:

$$\Delta\varepsilon_v(T) \sim 170 - 0.41T\ \text{meV}, \qquad (5)$$

which is shown as the blue line in Fig. 1(a). If Eq. (5) holds, $T_0 \sim 415$ K, and PbTe is an indirect-gap semiconductor

at the relevant temperatures. Coincidentally, in this case, $d\varepsilon_g/dT|_{T<420\,K} \sim d\Delta\varepsilon_v/dT$, which would pin the LVB to the CB.[26] There is no physical reason why this should be so: ε_g is dominated by spin-orbit interactions, and it is of very different physical origin than the LVB structure. In contrast to that, Eq. (4) gives $d\Delta\varepsilon_v/dT \sim 1/2 d\varepsilon_g/dT|_{T<420\,K}$, which pins the T dependence of the LVB to the mid-gap at the L-point. Under those circumstances, the physical origin of the T dependence of the direct-gap ε_g is clearly dissociated from that of $\Delta\varepsilon_v$. We now critique the existing experimental literature cited in support of either Eq. (4) or Eq. (5).

Compilations in Landolt-Börnstein[13] and Ravich's monograph[18] are consistent with Eq. (5), and $T_0 \sim 420$ K or at least $T_0 \leqslant 480$ K. The experimental evidence initially appears strong, because it consists of two independent measurements: optical measurements by Tauber *et al.*[26] and a strongly T-dependent Hall coefficient R_H, which has been confirmed experimentally by numerous authors, including coauthors of the present paper.[3] We address the two types of measurements.

In Ref. 26 high-temperature optical absorption data versus wavelength were extrapolated to zero, and these intercepts were interpreted as giving a net optical energy gap. This gap then appears to be T dependent following Eq. (1) up to about 400 K, above which the T dependence appears to vanish:[29] So for $T_0 \sim 400$ K, $(d\varepsilon_g/dT)_{T>T_0} = 0$, while $(d\varepsilon_g/dT)_{T<T_0} = 0.43 \pm 0.02$ meV K^{-1}, supporting Eq. (5). This interpretation was influenced by the behavior of $R_H(T)$ near the same temperature, which is discussed below. As already discussed in Ref. 12, because of (1) Fermi surface smearing, (2) the effect of indirect (L-Σ) optical transitions that require electron-phonon interactions, (3) the possible existence of Urbach tails, and (4) the strong and temperature-dependent nonparabolicity of the bands [Eqs. (1) and (2)], the interpretation of the high-temperature energy-dependent optical absorption curves becomes overly sensitive to both the energy range selected for the extrapolations and the assumptions made in the model used. To illustrate the point further, the optical absorption spectra of PbTe, PbSe, and PbS all show a similar temperature dependence,[30] yet only in PbTe are the results interpreted as above, and even then several different interpretations can be given to the same data, as can be seen by comparing Refs. 30 and 31. Ekuma *et al.*[32] and several older discussions of the optical data[19,33] show them to be compatible with Eq. (4), even if the older discussion may be prone to larger uncertainties.

Next, we review the literature on the temperature-dependent Hall coefficient $R_H(T)$. The nonmonotonic dependence of $R_H(T)$ in Na-doped PbTe has been the object of numerous investigations, some[18] of which conclude that the maximum in $R_H(T)$ near $T_0 \sim 415$ K identifies the LVB and UVB band-crossing ($\Delta\varepsilon_v = 0$) temperature [Eq. (5)], although this was not generally accepted in the old literature.[22] Here, we first point out that the literature used for $R_H(T)$ does not specify the field at which the transverse Hall resistivities were measured, only that it is fixed positive and negative fields. The field dependence is studied experimentally here. High-temperature measurements on heavily p-type doped material yield a negative slope to the field-dependent transverse Hall resistivity for $B < 0.5$T yet a positive slope for $B > 1.5$T. This provides evidence for the existence of an additional electron pocket that was ignored in the older analyses. The data[21,27] used to conclude that $T_0 \leqslant 480$ K show that $R_H(T > 400{-}550\,K) < 0$, which is attributed to the presence of intrinsic electrons thermally excited across the direct-gap ε_g. The authors of Ref. 21 do note that "the anomalously low temperature at which intrinsic conductivity appears is worthy of note," because, when such elemental calculations are repeated (see below), the influence of intrinsic electrons thermally excited across the gap only appears at temperatures much in excess of 500 K.

Secondly, the Hall coefficient R_H is related to the carrier concentration p through the Hall prefactor r_H in the relation $R_H = r_H/p.q$. The Hall prefactor itself is the product of two factors, the first ($\leqslant 1$) due to the anisotropy of the Fermi surface, and the second (which can be > 1) due to scattering. The prefactor r_H was not taken into account in the discussion of the evidence for Eq. (5), even though it had been determined experimentally[34] for group IV-VI rock salt semiconductors: r_H is shown to vary between 0.6 (in heavily p-type SnTe) and 1.7 (see below), and to have a very strong and non-monotonic dependence on doping level. A discussion of $r_H(p,T)$ is given by Allgaier.[24] Thirdly, we note that the maximum in $R_H(T)$ in a two-band system occurs when the conductance values of the two bands are equal, not when $\Delta\varepsilon_v = 0$; these conditions are not equivalent, because the LVB and UVB conductance values are functions of both carrier densities and mobilities, which can be expected to be very different in the two bands.

Finally, Airapetyants *et al.*[16] discusses the hole concentration dependence of the thermopower $S(p,T)$ (called a Pisarenko relation) at 300 K, alongside that of $R_H(p,T)$, and a summary of how he uses this to derive Eq. (4a) is given next. He assumes $r_H = 1$ to calculate the hole concentration value from Hall data, whereas experimentally[23] $1.1 < r_H < 1.7$ at these concentrations, so that his concentrations are underestimated by 10% to 70%. Below his value of $3{-}4 \times 10^{19}$ cm^{-3} holes, the data $S(p, T = 300\,K)$ match a Pisarenko relation $S_{UVB}(p_{UVB})$ calculated from the known band parameters of the UVB, but above that critical concentration, the experimental values for $S(p, T = 300\,K)$ saturate at about $50{-}55\,\mu$V/K. An analysis of the value of the thermopower $S_{UVB}(p_{UVB})$ at 300 K, using the band structure and equations in Ref. 18 and assuming acoustic phonon scattering, yields $S_{UVB}(p_{UVB} = 2 \times 10^{19}\,cm^{-3}, 300\,K) \sim 120\,\mu$V/K and $S_{UVB}(p_{UVB} = 5 \times 10^{19} cm^{-3}, 300\,K) \sim 50{-}55\,\mu$V/K. Above the doping level where the LVB starts getting filled, the thermopower does not continue on the Pisarenko relation $S_{UVB}(p_{UVB})$ of the UVB, but exceeds it, because $S(p)$ progressively moves from the Pisarenko relation of the UVB to that $S_{LVB}(p_{LVB})$ of the LVB, which lies higher ($S_{LVB}[p] > S_{UVB}[p]$) because the DOS of the LVB is larger than that of the UVB. This makes the thermopower $S(p)$ appear to saturate,[16] and the saturation value of the thermopower gives the hole concentration in the UVB when the Fermi energy is at the crossing point between UVB and LVB. The observed[16,18] saturation thermopower at 300 K around 50–55 μV/K therefore corresponds to a UVB that holds $p = 5 \times 10^{19}$ cm^{-3} holes when the Fermi energy reaches the LVB. Assuming the temperature dependence of Eq. (4), and using the values of Ref. 17 for the UVB, it is calculated to hold 5.2×10^{19} cm^{-3} holes at 300 K when the Fermi level reaches the LVB: Eq. (4) agrees with the

data of Airapetyants *et al.*[16] In contrast with the temperature dependence of Eq. (5), the UVB can only hold 1.9×10^{19} cm^{-3} holes at 300 K before the E_F reaches the top of the LVB [Fig. 1(b)]: Eq. (5) does not agree with the data of Airapetyants *et al.*[16] This calculation is also similar to that of Ref. 12, but the values for S in that reference are twice as high because they are calculated without taking into account the effect of electron scattering.

III. EXPERIMENTAL

Transport data are taken on $Pb_{0.99}Na_{0.01}Te_{1-x}S_x$ alloys with $x = 0$, 0.04, 0.08, 0.12, and $Pb_{1-y}Na_yTe_{0.92}S_{0.08}$ with $y = 0.01$, 0.005, 0.0025. A molar concentration of 0.01 in PbTe corresponds to $\sim 1.5 \times 10^{20}$ cm^{-3} atoms. Stoichiometric amounts of starting elements were loaded into carbon-coated quartz ampoules, which were then sealed under high vacuum. After heating the ampoules to 1373 K, they were annealed at 1100 K, thus generating single-phase material.[35] Powder x-ray diffraction confirms the single-phase nature, and the lattice constant decreases linearly with increasing sulfur content in accordance with Vegard's law.

In an orthonormal set of axes $[x,y,z]$, we apply a magnetic field B_z, and current or heat flux along x. Measurements are made of voltages along either x (longitudinal effects) or y (transverse effects), and temperature gradients along x. We measure electrical resistivity $\rho = \rho_{xx}$ and transverse Hall resistivity $\rho_{xy}(B_z)$ with a relative accuracy determined by the electrical noise in the signal of about 1×10^{-8} Ωm at a given temperature. The absolute accuracies of 3% on $\rho_{xy}(B_z)$ and 8% on $\rho_{xx}(B_z)$ are determined by the geometry of the sample. $\rho_{xy}(B_z)$ data yield the Hall coefficient $R_H = \lim_{B\to 0}(d\rho_{xy}(B_z)/dB_z)$. We measure the thermopower or Seebeck coefficient $S = S_{xx}$ with an accuracy near 3%, and the transverse isothermal Nernst–Ettingshausen thermopower $S_{xy}(B_z)$, which yields the isothermal Nernst–Ettingshausen coefficient $N = \lim_{B\to 0}(dS_{xy}(B_z)/dB_z)$with about 10^{-8} V K^{-1} T^{-1} accuracy. This is done over 77 K $\leqslant T \leqslant$ 620 K in a conventional flow cryostat in stepped temperature and magnetic field increments (-1.4T $\leqslant B \leqslant +1.4$T, and in some instances ± 1.8T). The low-field limit for the data is defined by the condition that $\mu B < 1$, here in practice $|B| < 0.5$T. The measured coefficient is the adiabatic Nernst coefficient, and the isothermal coefficient N is calculated by applying the standard correction.[36] The error analysis in these measurements is similar to that in Ref. 36. Measurements are extended to 2 K in a Quantum Design Physical Properties Measurement System (PPMS) using the AC Transport and Thermal Transport options (TTO). In this temperature range, the error in S is increased to over 5%, due to the size of the thermometry of the TTO and unquantifiable uncertainties in the software analysis. The high-temperature thermal conductivity $\kappa(T > 300\,\text{K})$ is deduced from measurements of the thermal diffusivity, α, in an Anter Corporation Flashline 3000, using the equation $\kappa = C_p\alpha\rho_d$, where ρ_d is the mass density, and C_p is the material specific heat. ρ_d is measured at 300 K using Archimedes's method and is adjusted over temperature for the literature values of the thermal expansion coefficient of PbTe.

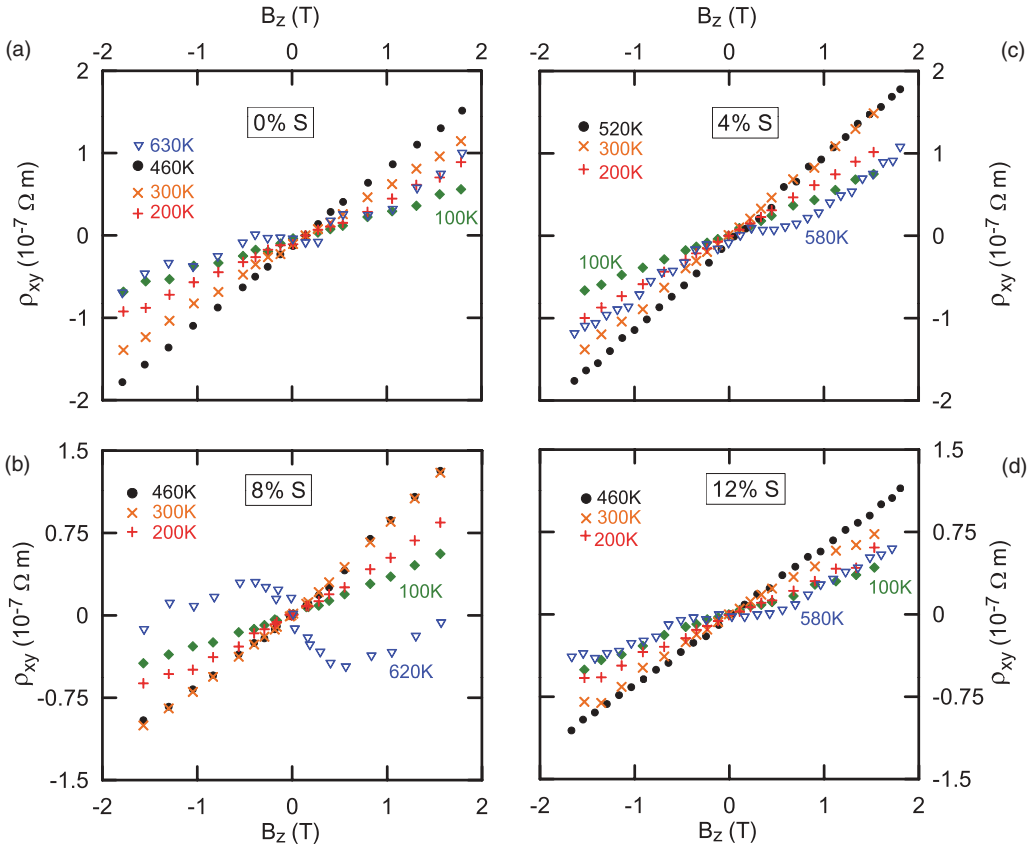

FIG. 2. (Color online) Hall resistivity $\rho_{xy}(B_z)$ as a function of magnetic field B_z for $Pb_{0.99}Na_{0.01}Te_{1-x}S_x$ at selected temperatures.

We measure C_p using the Heat Capacity Option in the PPMS (an absolute measurement) from 2 K to 300 K, and then from 300 K to 800 K in a Netzsch DSC 404-C at 20 °C min^{-1} under flowing Ar (<3% error) at Oak Ridge National Laboratory (ORNL). We renormalize the Netzsch C_p values over their entire temperature range by the ratio of the values obtained on both instruments at 300 K; this correction is less than 1%. High-temperature S (static DC method, <5% error) and ρ (4-wire method, 6% error) are also measured at ORNL in a ULVAC ZEM-2 under a static 0.09 MPa He exchange gas pressure, and using two R-type thermocouples and Ni electrodes.

IV. RESULTS

Traces of $\rho_{xy}(B_z)$ on $Pb_{0.99}Na_{0.01}Te_{1-x}S_x$ at a few selected temperatures are shown in Fig. 2. At $T \leqslant 400$ K, $\rho_{xy}(B_z)$ is linear with $d\rho_{xy}(B_z)/dB_z > 0$, but at $T \geqslant 600$ K, the low field $d\rho_{xy}(B_z)/dB_z$ is negative ($x = 0.08$) or has a plateau, while the high-field $d\rho_{xy}(B_z)/dB_z$ is positive and resumes a slope quite similar to that observed throughout the field range at $T \leqslant 400$ K. This behavior will be shown in the next section to be evidence for the appearance of a high-mobility electron in these samples at $T \geqslant 600$ K. By taking the value of $\rho_{xy}(B_z)$ at two fixed values of B_z of opposite polarity to deduce a pseudo-Hall coefficient R'_H defined as $R'_H \equiv [\rho_{xy}(B_z) - \rho_{xy}(-B_z)]/2B_z$, a quantity is derived that is not directly related to the carrier concentration because $p \neq 1/R'_H e$. The temperature dependence of R'_H is what was reported in the old literature and used as evidence for the bands crossing at $T_0 \sim 415$ K.

We show the galvanomagnetic properties from 80–420 K in Fig. 3 on the samples with $y = 0.01$. There is a plateau to R_H [Fig. 3(a)] for all samples at $T < 100$ K: at 80 K, taking $r_H = 0.65$,[22,23] $p = r_H/R_H q = 1.4 \times 10^{20}$ cm^{-3} for $x = 0.08$, which yields a doping efficiency of nearly unity (one Na atoms gives one hole). This varies slightly for the other samples with different x. Because $p > 1 \times 10^{20}$ cm^{-3}, one can calculate from the values for the UVB[17] that ε_F for all samples is in the LVB at all temperatures [Fig. 1(b)]. From 100–460 K, R_H increases greatly, and it can be seen from Fig. 2 that R_H turns negative at some $T > 460$ K; this trend is a similar to earlier reports,[21,37] and it is ascribed to the presence of additional electrons. This is in sharp contrast to the resonant PbTe-PbS : Tl[2,4] alloys, where R_H has almost no temperature dependence at the measured temperatures $\leqslant$420 K. There is no systematic trend in the magnitude of R_H with x: This most likely arises from unavoidable small variations in sample preparation due to the high reactivity of sodium and the necessity to anneal at 1100 K to achieve single-phase material; Crocker experienced similar issues when annealing at 1073 K.[23] Because of this, we do not compare absolute values of ρ [Fig. 3(b)] or Hall mobility (μ_H) as a function of

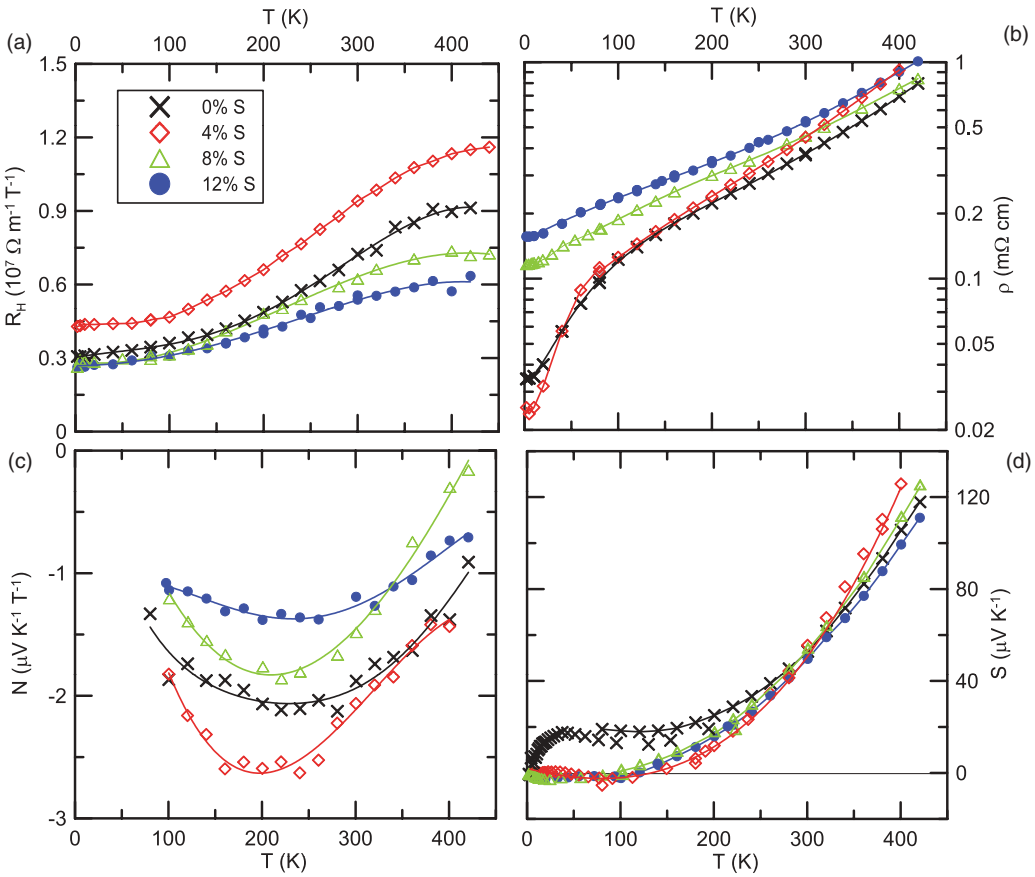

FIG. 3. (Color online) Low-temperature electrical properties of $Pb_{0.99}Na_{0.01}Te_{1-x}S_x$ samples from 2 to 420 K: (a) Hall coefficient, (b) electrical resistivity, (c) isothermal Nernst coefficient, and (d) thermopower. The symbols are experimental points; the lines are added to guide the eye.

x and p. The drop in ρ of the sample with $x = 0$ and 0.04 at ~60 K, which is absent in the others, is mentioned without explanation.

Moving to the thermomagnetic properties, also shown in Fig. 3, we notice that the Nernst coefficient N [Fig. 3(c)] is large for a heavily doped semiconductor. Rogers[38] also reports on N for a heavily Na-doped PbTe sample with similar 77 K R_H value: His temperature dependence is similar to that in Fig. 3, but the magnitude is roughly double; because it is not reported if that measurement concerns the isothermal or the adiabatic coefficient, which would explain the difference, no further analysis of the discrepancy is possible. The thermopower S [Fig. 3(d)] is ~53 μV/K at 300 K for all samples: This is the saturated value reported in Ref. 16 for all Na-doped samples where the ε_F presumably falls in the LVB. Below 140–120 K, S changes from positive to negative in sulfur-containing samples ($x > 0$), even though these are degenerately p-type doped materials.

An investigation of the low-temperature S and its magnetic field dependence (longitudinal field B parallel to heat flux) is shown in Fig. 4. For pure PbTe [$x = 0$, Fig. 4(a)], S is positive

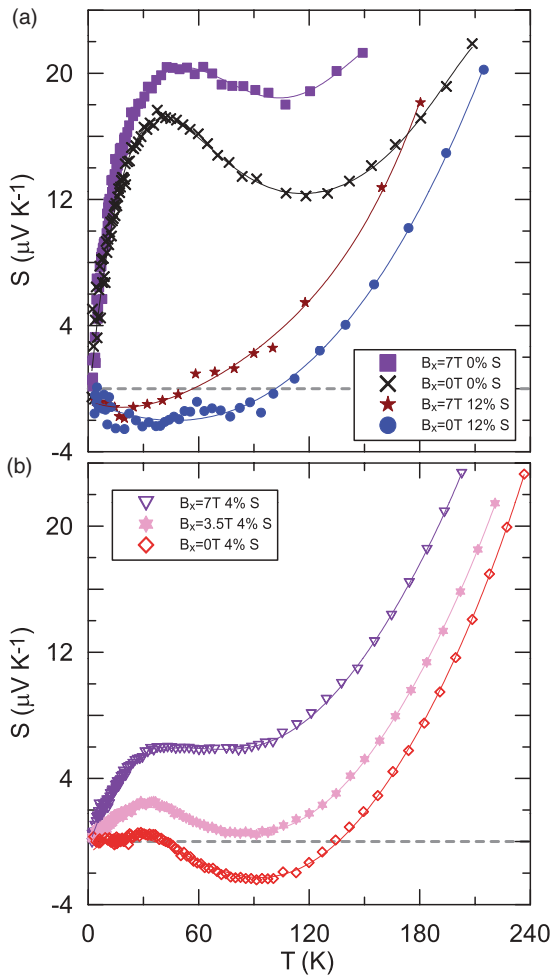

FIG. 4. (Color online) Thermopower from 2 to 240 K for $Pb_{0.99}Na_{0.01}Te_{1-x}S_x$ samples. (a) Data for sulfur concentrations $x = 0$ and $x = 0.12$ in 0 and 7 T field; (b) data for $x = 0.04$ in 0, 3.5 T, and 7 T field. The symbols are experimental points; the lines are added to guide the eye.

at all temperatures at 0 or $7T$. A maximum of 18 μV/K is reached at 40 K in zero field, most likely due to phonon drag. For $x = 0.04$, Fig. 4(b) reports that $S < 0$ at $T < 130$ K, with a small positive hump at 50 K, but it shows that with increasing magnetic field, the temperature range over which $S < 0$ progressively shrinks, so that the $7T$ curve qualitatively looks like the curves for $x = 0$. This can be viewed as a positive phonon-drag peak superimposed onto a magnetic-field–dependent diffusion thermopower that varies from negative at $0T$ for $T < 130$ K to positive at $7T$. For $x = 0.12$, there is a region with S negative at all fields, and the phonon-drag peak appears strongly reduced or absent. A further study of low-temperature $S(B,T)$, N, and R_H of $Pb_{1-y}Na_yTe_{0.92}S_{0.08}$ doped with $y = 0.01$, 0.005, 0.0025 is carried out in Fig. 5. This places ε_F at different locations in the valence band, with y and hole concentrations p. Table I shows the sodium concentration [Na], the saturated value of low-T Hall coefficient from Fig. 5(a), and the calculated hole concentration p using r_H from Ref. 23, illustrating that Na is a monovalent acceptor within the experimental error. Figure 5(b) shows the isothermal Nernst coefficient N, which has a minimum that increases in T with [Na]. Figure 5(c) shows that the T range where $S(H = 0,T) < 0$ is not a monotonic function of [Na]. As above, the effect of the magnetic field is to suppress the range where $S < 0$.

These samples match, within stated errors, the record values[1,3] reported for ZT in the p-type lead salt systems, as shown in Fig. 6. Here, the measurements of S, ρ, κ, and ZT on samples with $x = 0.08$ and 0.12 are extended to higher temperatures. The two samples have similar S, which for 300 K $< T <$ 600 K are linear with respect to temperature, and then peak at ~280 μV/K at 650 K; as is usual for PbTe,[16] ρ remains low, with a maximum of ~4.5 mΩ-cm for $x = 0.12$ at 700 K. Thermal conductivity shows a monotonic decrease with increasing sulfur content, presumably due to the reduction in lattice thermal conductivity. ZT reaches a value of ~1.55 at 700 K and remains above 1 at $T > 500$ K. The $ZT(T)$ from an $Pb_{97}Tl_2Na_1Te_{92}S_8$ alloy is also shown for comparison in Fig. 6(d), illustrating that its T dependence is different from that of Tl-free PbTe alloys. This, the difference in $R_H(T)$, and the increase above the Pisarenko relation demonstrate that the high ZT values in Tl-containing and Tl-free PbTe alloys have different physical origins.[2]

V. ANALYSIS

The simultaneous presence in these degenerately p-type doped semiconductors of a negative thermopower at the low-temperature end of the measurement range, and a negative Hall coefficient at the high-temperature end is, in our view, coincidental. From its magnetic field dependence, we conclude that the low-T thermopower is due to the energy dependence of the hole scattering mechanism. Indeed, $S(B = 0,T)$ is a function of the energy dependence of both band structure and scattering mechanisms. The latter is parameterized by writing the energy dependence of the relaxation time $\tau(\varepsilon)$ as a function of a scattering exponent λ defined generally by:

$$\lambda \equiv \partial \ln(\tau(\varepsilon))/\partial \ln(\varepsilon)|_{\varepsilon=\varepsilon_F} . \quad (6)$$

The scattering exponent is indicative of the electron scattering mechanism ($\lambda = -1/2$ for acoustic phonon

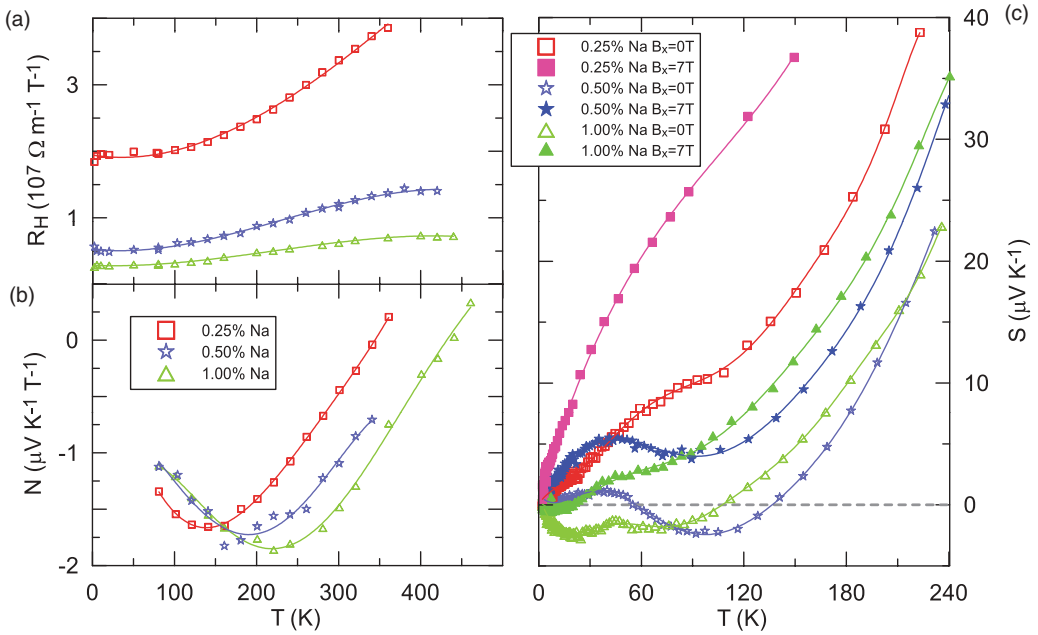

FIG. 5. (Color online) Low-temperature electrical properties of $Pb_{1-y}Na_yTe_{0.92}S_{0.08}$ samples with different sodium concentrations y indicated. (a) Hall coefficient, (b) isothermal Nernst coefficient, and (c) thermopower in 0 and 7 T longitudinal external magnetic field. The symbols are experimental points; the lines are added to guide the eye.

scattering, $\lambda = +1/2$ for polar optical phonon scattering above the Debye temperature, and $\lambda = 3/2$ for ionized impurity scattering). In contrast, the value of $\lim_{B\to\infty}(S[B,T])$ is scattering independent and a function of the band structure only.[18] Therefore, in the regime where $S(B=0,T) < 0$, the fact that $S(B \gg 1/\mu_H, T) > 0$ suggests that the dominant charge carrier is still holes. From this, and the fact that $S(B=0,T) < 0$, one concludes that the contribution of λ to $S(B=0,T)$ must be important enough to change its sign. To illustrate how λ can induce a sign reversal of S, one can write the expressions for the diffusion thermopower (excluding phonon-drag) for degenerately doped semiconductors with parabolic dispersions (such as the LVB of PbTe) as:[18]

$$S = \frac{2\pi^{3/2}}{3^{5/2}}\frac{k_B}{e}k_BT\frac{m^*_{\mathrm{DOS}}}{\hbar^2 p^{3/2}}\left(\lambda+\frac{3}{2}\right), \tag{7a}$$

whereas for a nonparabolic band (such as the UVB of PbTe):[18]

$$S = \frac{\pi^2}{3}\frac{k_B}{e}k_BT\frac{1}{\varepsilon_F}\left(\lambda+\frac{3}{2}-\frac{2\varepsilon_F/\varepsilon_G}{1+2\varepsilon_F/\varepsilon_G}+\frac{3}{2}\frac{\varepsilon_F/\varepsilon_G}{1+\varepsilon_F/\varepsilon_G}\right). \tag{7b}$$

In both cases, while for $\lambda = 0$ (the high-field limit) the sign of S will be that of the polarity of the charge carrier, when $\lambda < 0$, a sign reversal of the diffusion thermopower can be produced by the scattering mechanism. Because it is unlikely that acoustic phonon scattering ($\lambda = -1/2$) flips the sign of S, we propose that the negative thermopower is due to interband (L-Σ) scattering, since both valleys are occupied. In single-carrier systems, it is possible to deduce λ using the method of the four coefficients,[36] but here this approach applies only to the sample with $y = 0.0025$ at low T.

The four-coefficient[36] fits to the $y = 0.0025$ sample using the method of Ref. 36 give ε_F (80 K) = 83 meV and $m^*_{\mathrm{DOS}} = 0.22m_e$, both values consistent with the reported values for the UVB[17] and the measured hole density. They indicate that the scattering parameter (λ) increases monotonically with T. The values obtained at 80 K for $\lambda \sim -0.6$ are too negative for acoustic phonon scattering, suggesting a contribution from interband scattering. λ becomes positive above 200 K, indicating mostly acoustic phonon scattering with some optical phonon contribution. These concepts explain not only the observed magnetic field measurements, but also the quadratic dependence of S on temperature T, a unique feature in degenerately doped semiconductors, where usually $S \propto T^1$. The usual T^1 dependence is to be multiplied by an additional T dependence that originates from the increase of λ with T.

Besides the diffusion thermopower, phonon-drag acts on the majority carrier. Because we observe it to always have a positive contribution to the overall thermopower, this is another indication that the negative S does not arise from the presence of an unidentified electron pocket, reinforcing the conclusion

TABLE I. Sodium concentrations and Hall coefficients of $Pb_{1-y}Na_yTe_{0.92}S_{0.08}$.

Nominal Na concentration	[Na](10^{19} cm^{-3})	R_H(10^7 Ωm T^{-1})	r_H (Ref. 23)	$p = r_H/qR_H$(10^{19} cm^{-3})	$R_H(300)/R_H(80)$
0.25%	3.72	1.96	1.3	4.1	1.7
0.50%	7.44	0.52	0.65	7.8	2.3
1.00%	14.88	0.29	0.65	14	2.1

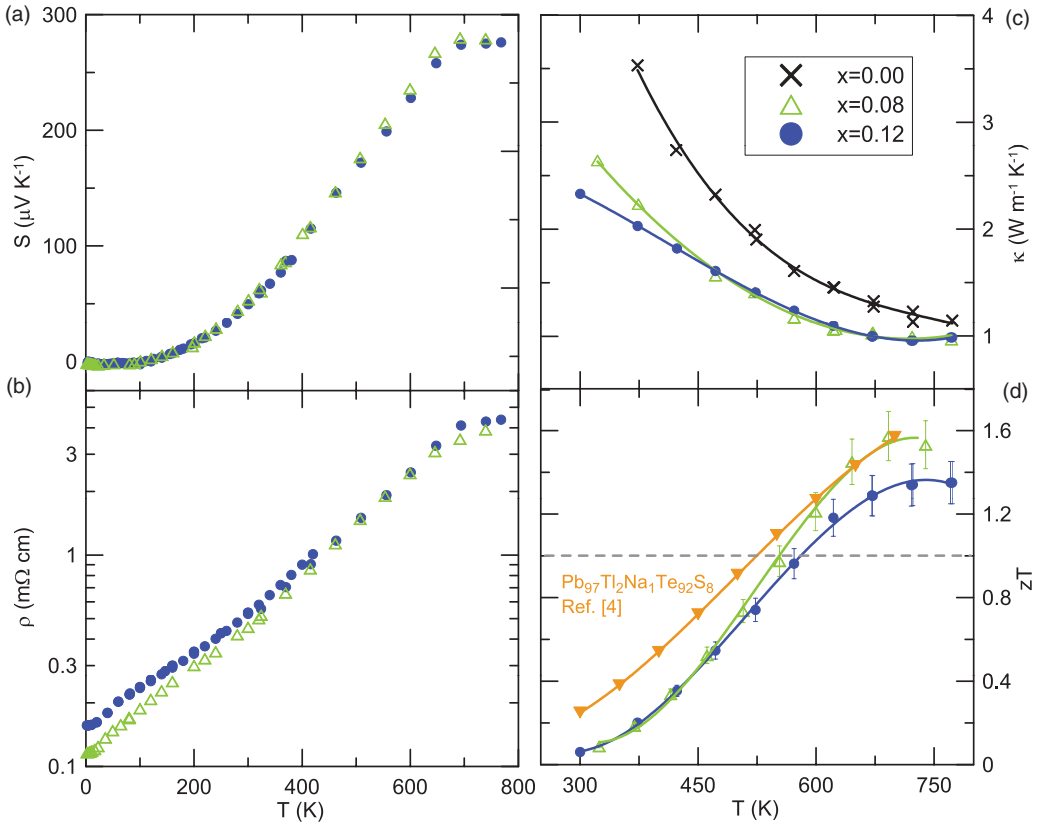

FIG. 6. (Color online) (a) Thermopower, (b) electrical resistivity, (c) thermal conductivity, and (d) ZT for $Pb_{0.99}Na_{0.01}Te_{1-x}S_x$ samples. The symbols are experimental points; the lines are added to guide the eye. The added ZT data are on a sample from Ref. 4 that contains the resonant impurity thallium.

that it must be related to a scattering effect. From Figs. 4 and 5, one can deduce that phonon-drag decreases with increasing sulfur content; this increases phonon-alloy scattering, which competes with phonon-electron interactions that give rise to phonon-drag. This explains why S never reaches negative values in heavily doped binary PbTe: The negative diffusion thermopower is likely also present, but it is masked by the large phonon-drag thermopower. Sulfur alloying may be needed to depress phonon-drag sufficiently to reveal the negative S.

Considering next the magnetic field dependence of the Hall conductance $\rho_{xy}(B_z)$ (Fig. 2), the fact that the high-temperature curves have two distinct slopes reveals the simultaneous presence of two carriers of opposite polarities, electrons and holes. In two-carrier systems (the electron concentration and mobility are denoted n and μ_e; the hole concentration and mobility p and μ_p) and in the presence of a transverse magnetic field B_z along the z axis, the longitudinal electrical resistivity $\rho_{xx}(B_z)$ and transverse Hall resistivity $\rho_{yx}(B_z)$ are the diagonal and off-diagonal elements of the equivalent conductivity elements $\sigma_{xx}(B_z)$ and $\sigma_{xy}(B_z)$, given as a function of the parameters above by:[39]

$$\sigma_{xx} = \frac{ne\mu_e}{1+\mu_e^2 B_z^2} + \frac{pe\mu_h}{1+\mu_h^2 B_z^2}, \quad \sigma_{xy} = -\frac{ne\mu_e^2 B_z}{1+\mu_e^2 B_z^2} + \frac{pe\mu_h^2 B_z}{1+\mu_h^2 B_z^2}$$
$$\rho_{xx} = \frac{\sigma_{xx}}{\sigma_{xx}^2+\sigma_{xy}^2}, \quad \rho_{xy} = \frac{\sigma_{xy}}{\sigma_{xx}^2+\sigma_{xy}^2}. \tag{8}$$

At an arbitrary field, $\rho_{yx}(B_z)$ is no longer a linear function of B_z, and $d\rho_{yx}/dB_z$ can change sign with B_z. The low-field Hall coefficient R_H is the low-field slope of $\rho_{yx}(B_z)$:

$$R_H \equiv \lim_{B_z\to 0}\left(\frac{d\rho_{xy}}{dB_z}\right) = \frac{-n\mu_e^2 + p\mu_h^2}{n\mu_e + p\mu_h}, \tag{9}$$

while the high-field limit, Eq. (9), gives:

$$\lim_{B_z\to\infty}\left(\frac{d\rho_{xy}}{dB_z}\right) = \frac{1}{p-n}. \tag{10}$$

From Eq. (9), we conclude that the low-field Hall resistivity $\rho_{yx}(B_z)$ is most sensitive to the presence of high-mobility minority carriers, and more so than the thermopower, which is given by $S = \frac{-S_e n\mu_e + S_h p\mu_h}{n\mu_e + p\mu_h}$, where S_e and S_p are for electrons and holes, respectively. In contrast, the high-field $\rho_{yx}(B_z)$ measures the net carrier concentration and is representative of the majority carrier concentration when $p \gg n$. Figure 2 is therefore characteristic of a semiconductor that is dominantly p-type, but in which a low concentration of high-mobility electrons appears around 600 K. One cannot deduce from Fig. 2 what electrons these are. Andreev[21] makes similar observations and reaches the same conclusion but suggests that the high-mobility minority electrons could be thermally activated in the L-point CB, although he expresses doubts about his own suggestion (see introduction). Figure 7(a) reports the results for the calculation of the density of extrinsic holes (x axis) and thermally activated electrons (y axis)

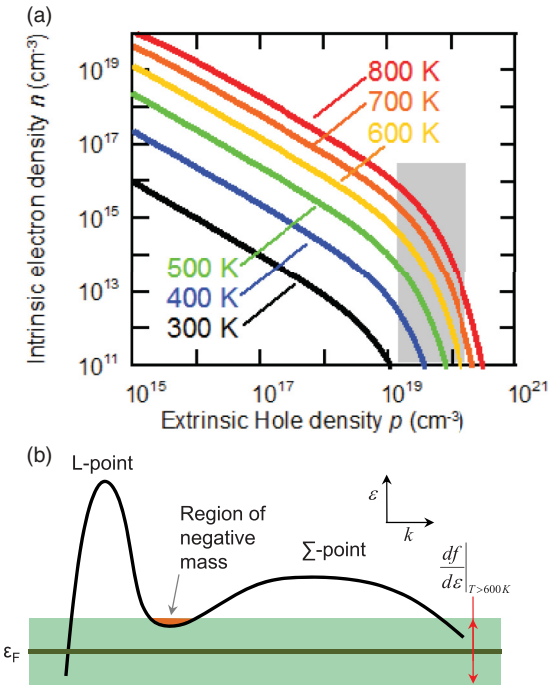

FIG. 7. (Color online) (a) Calculated thermally excited electron concentration at various temperatures as a function of hole carrier concentration. The gray band indicates the range of extrinsic hole densities in samples studied. (b) The valence band of PbTe alloys contains multiple pockets when the samples are lightly doped p-type: The hole Fermi surface is then multiply connected. When the Fermi level ε_F is lowered by doping to the level shown here, these multiple pockets merge into one singly connected complex Fermi surface. The green band represents the width at half maximum of the energy derivative $df/d\varepsilon$ of the Fermi distribution function f at 600 K. When this band encompasses the regions in the dispersion relation $\varepsilon(\mathbf{k})$, where the upper valence bands, near the L-points of the Brillouin zone, touch the lower valence bands centered near the Σ-points, thermally excited carriers (orange) appear in parts of the Brillouin zone where the dispersion $\varepsilon(\mathbf{k})$ has curvature of polarity opposite to that of the holes. The thermally excited carriers in that orange region behave like electrons under the influence of an external electric field.

in PbTe using Fermi statistics,[40] the temperature-dependent $m^*_{\mathrm{DOS}}(p,T)$, $\varepsilon_g(T)$, and $\varepsilon_F(p)$ band structure parameters of PbTe,[17] and the non-parabolicity of the dispersion relations.[36] The hatched region gives the doping range of our samples: at 600 K, no more than 10^{16} cm^{-3} electrons can be present in the L-point CB, while the low-field negative slope in Fig. 2(a) corresponds to the mid-10^{19} cm^{-3} electron concentration range. This discrepancy by over three orders of magnitude suggests that these electrons are not simply thermally activated across ε_g into the L-point CB, the discrepancy noted by Andreev.[21]

We suggest that the electron-like behavior is of topological origin and arises from the regions in k-space where the pieces of the hole Fermi surfaces centered around the L- and Σ-points touch. The hole Fermi surface of low-doped p-type PbTe is topologically multiply connected, consisting of four ellipsoid-like pockets centered at the L-point, and eight centered at the Σ-points. When the doping level is increased, each of these pockets increases in volume until they touch: Now the entire Fermi surface is singly connected. This situation, illustrated in Fig. 7(b), shows that "necks" (regions of inverted curvature) are induced by this change in topology of the band structure at the points where the different pockets touch. These regions will have a curvature of opposite polarity of the majority holes (L-W axis; Fig. 1 of Ref. 12); in response to a force induced by a potential or temperature gradient, they will respond as electrons. This latter effect is well known in the Fermi surface of copper, which is mostly a sphere. Because the Fermi sphere of copper is just a little too large to fit inside the first Brillouin zone, "necks" develop at the points where the spheres of adjacent Brillouin zones touch. Although each copper atom gives one electron to the solid, the necks have transport properties of holes. The positive thermopower of copper is explained by the presence of these topological holes. The samples in this study are sufficiently doped that ε_F falls below the maximum of the LVB [see Fig. 7(b)], so that the topological electrons do not exist at low temperature. When the temperature is increased sufficiently that the region of negative curvature comes within k_BT from ε_F, electron-like transport properties arise. Notice also that the thermopower saturates at 700 K [Fig. 6(a)], where the density of intrinsic electrons at L-point is $\leqslant 10^{16}$ cm^{-3} [Fig. 7(a)]: this is likely another manifestation of the topological electrons seen in $\rho_{xy}(B_z)$. As explained above, the fact that the Hall coefficient turns negative and the thermopower remains positive is an indication that the topological electrons have a high mobility.

An alteration in properties due to the formation of an impurity band, possibly because of an inhomogeneous distribution throughout the samples of either S or Na atoms, is also possible. It is less likely to contribute much to $\rho_{xy}(B_z)$, however, because such a band is unlikely to have a mobility higher than that of the holes near the Σ-points.

VI. SUMMARY AND CONCLUSIONS

The results presented here are on material with ZT values reaching ~1.55 at 700 K. We demonstrate that the temperature dependence of the Hall coefficient of heavily p-type doped PbTe, which was used as evidence in the literature for a crossing of two valence bands in PbTe at ~415 K, is due to another cause, namely, the appearance of an additional electron contribution. Complete magnetic-field–dependent Hall-resistivity data must be taken into account to derive the proper carrier concentrations. The previously suggested temperature-induced rapid rise in energy of the "heavy" hole LVB relative to the "light" hole UVB[6] is not supported by the present experimental data. The temperature dependence posited by Allgaier and Houston[25] and Airapetyants[16] is more plausible, and the energy overlap between LVB and UVB has a temperature dependence of $\mathrm{d}\Delta\varepsilon_v/\mathrm{d}T = -0.2$ (meV K^{-1}), which is about one half of the temperature dependence of the direct energy gap $\mathrm{d}\Delta\varepsilon_v/\mathrm{d}T \sim 1/2\mathrm{d}\varepsilon_g/\mathrm{d}T|_{T<420\,\mathrm{K}}$. Combining this with the low-temperature ($T \leqslant 80$ K) value of $\Delta\varepsilon_v = 160-170$ meV from the literature compiled by Ravich *et al.*[18] leads to the further conclusion that PbTe continues to be a direct-gap semiconductor at temperatures where the ZT and $S^2\sigma$ of p-type PbTe are optimal, e.g., 700–800 K. This does not detract from the fact that the heavy holes contribute dominantly

to the ZT of lead-salt–based semiconductors doped in the high–10^{19} cm^{-3} range.

The low-temperature diffusion thermopower is negative below about 130 K, and magnetothermopower measurements show that that this is due to scattering, possibly interband scattering between the LVB and UVB. The qualitative differences between the temperature dependencies of the $ZT(T)$ of materials where the electronic properties are dominated by the heavy valence band, and the $ZT(T)$ of Tl-doped PbTe are also shown.

ACKNOWLEDGMENTS

This work is supported as part of the Center for Revolutionary Materials for Solid State Energy Conversion, an EFRC funded by the US DOE, Office of Science, Office of Basic Energy Sciences under Award Number DE-SC0001054. The authors would also like to acknowledge collaboration through the same EFRC with Oak Ridge National Laboratory managed by the UT-Battelle LLC, for the Department of Energy under Contract No. DE-AC05000OR22725.

[1] Y. Pei, X. Shi, A. LaLonde, H. Wang, L. Chen, and G. J. Snyder, Nature **473**, 66 (2011); K. Biswas, J. Q. He, G. Y. Wang, S. H. Lo, C. Uher,V. P. Dravid, and M. G. Kanatzidis, Energy Environ. Sci. **4**, 4675 (2011); K. Biswas, J. Q. He, Q. C. Zhang, G. Y. Wang, C. Uher, V. P. Dravid, and M. G. Kanatzidis, Nature Chemistry **3**, 160 (2011).

[2] J. P. Heremans, V. Jovovic, E. S. Toberer, A. Saramat, K. Kurosaki, A. Charoenphakdee, S. Yamanaka, and G. J. Snyder, Science **321**, 554 (2008).

[3] S. N. Girard, J. He, X. Zhou, D. Shoemaker, C. M. Jaworski, C. Uher, V. Dravid, J. P. Heremans, and M. Kanatzidis, J. Am. Chem. Soc. **133**, 16588 (2011).

[4] C. M. Jaworski, B. Wiendlocha, V. Jovovic, and J. P. Heremans, Energy Environ. Sci. **4**, 4155 (2011).

[5] L. E. Bell, Science **321**, 1457 (2008).

[6] Y. Pei, A. LaLonde, S. Iwanaga, and G. J. Snyder, Energy Environ. Sci. **4**, 2085 (2011).

[7] A. LaLonde, Y. Pei, and G. J. Snyder, Energy Environ. Sci. **4**, 2090 (2011).

[8] E. S. Bozin, C. D. Malliakas, P. Souvatzis, T. Proffen, N. A. Spaldin, M. G. Kanatzidis, and S. J. L. Billenge, Science **330**, 1660 (2010).

[9] O. Delaire, J. Ma, K. Marty, A. F. May, M. A. McGuire, M.-H. Du, D. J. Singh, A. Podlesnyak, G. Ehlers, M. D. Lumsden, and B. C. Sales, Nat. Mater. **10**, 614 (2011).

[10] M. D. Nielsen, V. Ozolins, and J. P. Heremans, Energy Environ. Sci. DOI: 10.1039/C2EE23391F (2013).

[11] Kh. A. Abdullin, A. I. Lebedev, A. M. Gas'kov, V. N. Denim, and V. P. Zlomanov, JETP Lett. **40**, 998 (1984).

[12] D. J. Singh, Phys. Rev. B **81**, 195217 (2010).

[13] O. Madelung (ed.), *Landolt-Börnstein: Numerical Data and Functional Relationships in Science and Technology*, new series, Vol. 17, subvolume f (Springer, Berlin, 1983).

[14] M. K. Zhitinskaya, V. I. Kaidanov, and I. A. Chernik, Sov. Phys. Solid State **8**, 246 (1966).

[15] C. M. Jaworski and J. P. Heremans, Phys. Rev. B **85**, 033204 (2012).

[16] S. V. Airapetyants, M. N. Vinogradova, I. N. Dubrovskaya, N. V. Kolomoets, and I. M. Rudnik, Sov. Phys. Solid State **8**, 1069 (1966).

[17] H. Preier, J. Appl. Phys. **20**, 189 (1979).

[18] Y. I. Ravich, *Semiconducting Lead Chalcogonides* (Plenum Press, New York, NY, 1979), and references therein.

[19] L. M. Rogers, Br. J. Appl. Phys. **18**, 1227 (1967).

[20] Y. I. Ravich and S. A. Nemov, Phys. Usp. **41**, 735 (1989).

[21] A. A. Andreev and V. N. Radionov, Sov. Phys. Sem. **1**, 183 (1967); A. A. Andreev, Sov. Phys. Solid State **8**, 2256 (1967).

[22] A. J. Crocker, J. Phys. Chem. Solids **28**, 1903 (1967).

[23] A. J. Crocker and L. M. Rogers, J. Phys. Colloques **29**, C4-129 (1968).

[24] R. S. Allgaier, Phys. Rev. **119**, 554 (1960); J. Appl. Phys. **32**, 2185 (1961).

[25] R. S. Allgaier and B. B. Houston, J. Appl. Phys. **37**, 302 (1966).

[26] R. N. Tauber, A. A. Machonis, and I. B. Cadoff, J. Appl. Phys. **37**, 4855 (1966).

[27] N. V. Kolomoets, M. N. Vinogradova, E.Ya. Lev, and L. M. Sysoeva, Sov. Phys. Solid State **8**, 2237 (1966).

[28] A. A. Andrevv, J. Phys. Colloques **29**, C4-50 (1968).

[29] H. Sitter, K. Lischka, and H. Heinrich, Phys. Rev. B **16**, 680 (1977).

[30] A. F. Gibson, Proc. Phys. Soc. B **65**, 378 (1952).

[31] R. A. Smith, Physica **20**, 910 (1954).

[32] C. E. Ekuma, D. J. Singh, J. Moreno, and M. Jarrell, Phys. Rev. B **85**, 085205 (2012).

[33] J. R. Dixon and H. R. Riedl, Phys. Rev. **138**, A873 (1965).

[34] R. Tsu, W. E. Howard, and L. Esaki, Phys. Rev. **172**, 779 (1968); this article further reports the variation of r_H when the Fermi level enters the heavy hole band of SnTe.

[35] H. Lui and Y. Y. Chang, Mineral. Mag. **58**, 567 (1994).

[36] J. P. Heremans, C. M. Thrush, and D. T. Morelli, Phys. Rev. B **70**, 115334 (2004).

[37] A. J. Crocker and L. M. Rogers, Br. J. Appl. Phys. **18**, 563 (1967).

[38] L. M. Rogers, Br. J. Appl. Phys. **1**, 1067 (1966).

[39] V. Jovovic and J. P. Heremans, Phys. Rev. B **77**, 245204 (2008).

[40] J. S. Blakemore, *Semiconductor Statistics* (Dover Publications, Mineola, NY, 1987).